Published as:
Sun, P., Chen, Q., Fu, C., Xu, Y., Sun, R., Li, J., Yu, H., Zhang, C., Liu, Y., Ye, Z., Tian, Y., Heino, M., 2020. Latitudinal differences in early growth of largehead hairtail (Trichiurus japonicus) in relation to environmental variables. Fisheries Oceanography 29, 470–483. doi:10.1111/fog.12490

Latitudinal differences in early growth of largehead hairtail (*Trichiurus japonicus*) in relation to environmental variables

Peng Sun[1,2], Qi Chen[1], Caihong Fu[3], Yi Xu[4], Runlong Sun[1], Jianchao Li[1], Haiqing Yu[1], Chi Zhang[1], Yang Liu[1], Zhenjiang Ye[1], Yongjun Tian[1,5,6*], Mikko Heino[2,7,8]

[1] *College of Fisheries, Ocean University of China, Qingdao, China*

[2] *Department of Biological Sciences, University of Bergen, Bergen, Norway*

[3] *Fisheries and Oceans Canada, Pacific Biological Station, Nanaimo, Canada*

[4] *Fisheries and Oceans Canada, Fraser River Stock Assessment, Delta, Canada*

[5] *Laboratory for Marine Fisheries Science and Food Production Processes, Pilot National Laboratory for Marine Science and Technology, Qingdao, China*

[6] *Frontiers Science Center for Deep Ocean Multispheres and Earth System (FDOMES), Ocean University of China, Qingdao, China*

[7] *Institute of Marine Research, Bergen, Norway*

[8] *Evolution and Ecology Program, International Institute for Applied Systems Analysis, Laxenburg, Austria*

**Corresponding Author: tel: +86-532-82033378; e-mail: yjtian@ouc.edu.cn.*

Abstract

Largehead hairtail (*Trichiurus japonicus*) in the China Seas shows an increasing catch trend, despite continued overexploitation, which could be attributed to improved recruitment as a result of strengthened early growth. To understand the early growth variability of largehead hairtail, we examined the linkages between early growth, as revealed by otolith microstructure, and the associated environmental variables over both spatial and temporal scales. Young-of-the-Year largehead hairtail were collected from three regions in the Bohai, Yellow and East China Seas between 29°–39° N. Daily increment widths of sagittal otoliths were measured and used as a proxy for somatic growth. We found two spawning cohorts, Spring- and Summer-spawned cohorts, that showed latitudinal differences in both mean growth and growth pattern. The transition time from larval to juvenile stage was identified at around 40 days. Daily increment widths of two cohorts showed similar growth pattern in the first 40 days, while location had a marked effect on daily growth over 41–110 days. This suggests physiologically constrained growth pattern in larval stage, but more plastic growth subject to habitat-specific influences in juvenile stage. The gradient forest analysis identified sea bottom temperature, vertical temperature gradient and sea surface salinity, as the most important variables in determining early growth. Latitudinal differences in early growth pattern and their response to environmental variables suggest adaptive plasticity of early growth, which has notable implication for the management and sustainable utilization of this important but heavily exploited resource in the China Seas.

Keywords: largehead hairtail; early growth pattern; otolith microstructure analysis; habitat- and

37 stage-specific growth; generalized additive mixed model; gradient forest analysis; China Seas

Introduction

An important commercial fish species in the China Seas, largehead hairtail (*Trichiurus japonicus*) is characterized by wide distribution from the Bohai Sea, Yellow Sea to the East China Sea; these areas account for more than 85% of the Chinese catches (Xu and Chen, 2015). The catch of largehead hairtail has been on the rise in the Bohai Sea, Yellow Sea and East China Sea (Zhang, 2004; Wang *et al.*, 2011; Xu and Chen, 2015). At the same time, the population characteristics of largehead hairtail have changed, i.e. the catch is largely composed of 1-year-old fish, and the stock is characterized by early maturation, prolonged spawning season and increased number of young fish, which may indicate increased recruitment (Lin *et al.*, 2006). These demographic characteristics can compensate the negative effects from high fishing pressure. The mean pre-anal length and pre-anal length at maturity of largehead hairtail have decreased while the growth parameters and exploitation rate had increased in the past, which suggests that the ecological strategy of largehead hairtail may have changed (Ji *et al.*, 2019).

We hypothesized that the adaptive capacity of early growth in largehead hairtail has contributed to its continued reproductive success, allowing it to persist and even prosper under continued high fishing pressure and environmental change. Reproductive success is closely related with long-term population stability, particularly under disturbances such as fishing pressure (Stearns, 1992; Neubauer *et al.*, 2013; Lowerre-Barbieri *et al.*, 2017). In fish populations, recruitment variability is mainly determined by survival and growth patterns during the larval and juvenile stages (Houde, 1989; Köster *et al.*, 2003; Baumann *et al.*, 2006). A better understanding of the early growth process of largehead hairtail from larval to juvenile stage, and the associated environmental effects,

is desired to explain the recruitment of this economically and ecologically important fish species.

In most marine fish populations reproduction is characterized by high fecundity and subsequent high mortality during early life stages (Bailey and Houde, 1989; Houde and Zastrow, 1993; Otterlei *et al.*, 1999). Because variation in early growth rate is closely related to early life stage mortality, early growth plays an important role in determining recruitment and subsequent adult populations (Houde, 1987; Cowen and Sponaugle, 2009; Munday *et al.*, 2009; Lett *et al.*, 2010; Takahashi *et al.*, 2012; Watanabe *et al.*, 2014). While early growth variation can be inherent, it can also be influenced by environmental variability, i.e., growth plasticity, which can have an important influence on recruitment and eventually population dynamics (e.g. Wullschleger and Jokela, 1999; Scharsack *et al.*, 2007). Previous studies based on long-term catch data of largehead hairtail in the East China Sea have shown that both fishing and climate change have influenced the largehead hairtail population dynamics (Chen *et al.*, 2004; Wang *et al.*, 2011). The growth rate and survival of populations are influenced by physical and biological factors, such as food availability and environmental variables (e.g., Miller *et al.*, 1988; Buckel *et al.*, 1995; Tupper and Boutilier, 1995; Denit and Sponaugle, 2004; Sogard, 2011). Food availability, which may be influenced by stratification and ocean currents (especially upwelling), has an important role in affecting the growth and survival of early life stages as well as fish population dynamics and ecosystems (e.g. Hjort, 1914; Ljunggren *et al.*, 2010; Morgan *et al.*, 2013; Mallo *et al.*, 2016; Schismenou *et al.*, 2016; Rozema *et al.*, 2017; Koenker *et al.*, 2018). Temperature is generally considered to be one of the most important environmental variables in early growth of fish populations. It has a significant influence on not only the timing and duration of fish spawning season, but also primary production

in an ecosystem (Houde, 1989; Morse, 1989; Bergenius *et al.*, 2002; Valenzuela and Vargas, 2002; Husebø *et al.*, 2007; Trip *et al.*, 2014; Gallagher *et al.*, 2015; Fedewa *et al.*, 2017). Primary production, represented by chlorophyll concentration, is used as an indicator of food availability in most studies (Bailey and Houde, 1989; Leggett and Deblois, 1994).

Individuals hatching at different times and regions may experience different environmental conditions, which may affect their growth and subsequent survival (Kingsford and Hughes, 2005; Ruttenberg *et al.*, 2005; Hughes *et al.*, 2017). In this study, three sampling areas cover the Bohai Sea, Yellow Sea and East China Sea, over a large latitudinal range of 29° to 39° N. In the Bohai Sea, the Yellow River effluents may have an important influence on environmental conditions and food availability (Gu and Xiu, 1996; Yang *et al.*, 2011). The Yellow Sea Cold Water and Yellow Sea Warm Currents are two important hydrological processes in the Yellow Sea, which may have a great impact on the spatial-temporal variation of water temperature and salinity. Similarly, Taiwan Warm Current, Kuroshio, and Yangtze River Runoff play important roles in the East China Sea (Li *et al.*, 2006; Bao *et al.*, 2010; Wang *et al.*, 2011; Mi *et al.*, 2012). As a widely distributed species, largehead hairtail may inhabit and experience different sea areas with large latitudinal differences. Although largehead hairtail undergo seasonal migration, such migration does not commence until after the early life stage (e.g. Liu *et al.*, 2009; Xu and Chen, 2015). Therefore, it is essential to explore the influence of environmental variables among three sea areas on early growth of largehead hairtail.

A previous study about early growth of largehead hairtail based on otolith microstructure analysis has already confirmed that largehead hairtail spawn almost year-round, with two dominant

spawning periods in the East China Sea (Sun *et al.*, 2020). Here we extend that study by including two more sampling regions (Bohai Sea and Yellow Sea) as well as further samples from the East China Sea. The main objectives of this study are to (1) explore latitudinal differences in early growth of largehead hairtail as revealed by otolith microstructure, (2) identify linkages between the early growth and associated environmental variables on both spatial and temporal scales, (3) advance understanding of the largehead hairtail population dynamics to explain the reasons for the sustained high yield of largehead hairtail under long-term high fishing pressure in the China Seas.

Materials and methods

Study collection

Young-of-the-Year (YoY) largehead hairtail were collected from three regions in the China Seas: Dalian (DL), Qingdao (QD) and Zhoushan (ZH), representing the Bohai Sea, Yellow Sea and East China Sea, respectively (Fig. 1). Sampling was conducted with stow nets, a fixed-position fishing gear with a total stretched length of approximately 90 m mouth circumference of 1380 meshes and mesh size of 17 mm. Sampling effort was concentrated in fall 2017, with some additional sampling in summer 2017 and spring 2018; we attempted to obtain monthly samples but fishing restrictions limited sampling especially in summer. Table 1 summarizes the detailed sampling information.

Otolith analysis

In the laboratory, a total of 260 YoY largehead hairtail were measured for total length, pre-anal length, dorsal fin-anus length, body height, total weight and gonad weight. Sagittal otoliths were

122 removed, cleaned and saved in 75% ethanol. Right otoliths were selected to be embedded
123 individually in epoxy resin (Spurr, 1969; Baumann *et al.*, 2003). Transverse sections (~500 μm
124 thick) through the primordia of otoliths were obtained using an IsoMet saw (Buehler Ltd), mounted
125 on microscope slides, and sectioned with a series of 600 to 4200 grit sandpapers and alumina
126 powder on micropolishing cloth (Stevenson and Campana, 1992; Neuman *et al.*, 2001). Both sides
127 of the otoliths were ground and polished to remove the cutting marks of the saw until all increments
128 could be distinguished and counted. Photographs were taken under 200× magnification using an
129 Olympus microscope coupled with an optical camera system. Daily ages and increment widths were
130 estimated using the Image J image processing and analysis software (http://imagej.nih.gov/ij/) along
131 the same axis, from core to ventral of the otolith (Fig. 2). Each otolith was read independently thrice
132 by the same reader following the guideline by Whitman and Johnson (2016); the last reading was
133 chosen based on the assumption of a positive learning curve. If the three readings of an otolith were
134 different from each other by more than 5%, the readings would be rejected and the otolith was
135 re-read. The precision of age determination was estimated using the coefficient of variation method
136 provided in Campana (2001).

137 In this study, we hypothesized that daily rings are formed after the onset of exogenous feeding,
138 like in many other fish species (e.g., Shoji, 2005; Baumann *et al.*, 2006; Mesa, 2007; Johnson *et al.*,
139 2007). Because estimates of the first feeding day after hatching are lacking for largehead hairtail,
140 we treated the first daily ring of otolith as corresponding to the age of one day. Hatching dates were
141 then back-calculated based on capture dates and age estimates.

142 **Environmental variables**

The daily estimates of environmental variables, including sea surface salinity (SSS), sea surface temperature (SST), sea bottom temperature (SBT), difference between sea surface and bottom temperature (TD), and eastward and northward velocities (*u* and *v*), were derived from the daily product published by the Copernicus Marine Environment Monitoring Service (Product: GLOBAL_ANALYSIS_FORECAST_PHY_001_024; Data can be downloaded from the website: ftp://nrt.cmems-du.eu/Core/GLOBAL_ANALYSIS_FORECAST_PHY_001_024/global-analysis-forecast-phy-001-024). The physical ocean model for this product is NEMO that has 50 vertical levels ranging from 0 to 5500 meters (the vertical coordinate system was set as the z-coordinate with full step bathymetry and has 22 layers in the upper 100 meters) and a 1/12 degree horizontal resolution. The meteorological forcing of the ocean model is ECMWF ERA-Interim reanalysis (3-hourly). And meanwhile the satellite derived sea-surface height anomaly and SST (spatial resolution: 1/4 degree; Donlon *et al.*, 2012) were assimilated to improve model performance. These variables were spatially integrated to represent the daily change in three sampling regions (Fig. 1).

Spawning cohorts

For consistency and ease of comparisons among the three sampling regions, we divided the specimens into two spawning cohorts based on their back-calculated hatching date (Fig. 3). Specimens hatched within the same period were defined as a spawning cohort. We chose to use 40-day temporal window as a trade-off between large enough sample size and sufficiently narrow temporal scope. Thus, the hatching dates of the Spring-spawned cohort were defined as 3/11/2017–4/18/2017 in DL, 3/16/2017–4/26/2017 in QD, and 3/1/2017–3/27/2017 in ZH, and those of the Summer-spawned cohort as 6/18/2017–7/28/2017 in DL, 7/10/2017–8/9/2017 in QD, and

6/9/2017–7/20/2017 in ZH. These definitions gave sample sizes of N=15, 34, and 20 for the Spring-spawned cohort in respectively DL, QD, and ZH, and N=28, 37, and 23 for the Summer-spawned cohort in the same regions. YoY largehead hairtail are not migratory before spawning and inhabit mostly the coastal area (Xu and Chen, 2015), so the increment widths were averaged over individuals to obtain date- and region-specific estimates.

Statistical analysis

Our previous study shows that the accumulated otolith daily increments are significantly linearly correlated with pre-anal length (Sun *et al.* 2020), suggesting that otolith daily increments width of the YoY largehead hairtail represent well the individual somatic growth. In this study we used Generalized Additive Mixed Models (GAMM, Lin and Zhang, 1999; Rupert *et al.*, 2003; Zuur *et al.*, 2009; Wood, 2019) to relate daily increment with factors that influence the growth pattern of specimens. GAMM, an extension of generalized additive models, is a fixed-effects regression model with additional random-effect terms and with unknown smooth functions for the covariates, which make it appropriate for analyzing data with a nonlinear age-dependence (Rupert *et al.*, 2003; Zuur *et al.*, 2009). In order to evaluate the effect of location (i.e., DL, QD and ZH) on daily increment widths, two GAMM models were compared:

Model1: $\log(IW_{i,j}) \sim Location_i + s(Age_{i,j}) + \varepsilon_i$

Model2: $\log(IW_{i,j}) \sim Location_i + s(Age_{i,j}, Location_i) + \varepsilon_i$

where $IW_{i,j}$ is the width of j^{th} daily increment of individual *i*, Location represents sampling region (DL, QD or ZH), s() is the smoothing function, Age is age at formation of increment *j*, and ε_i is an individual-level random effect. To avoid over-fitting, the extent of flexibility was restricted to a

maximum of 8. Model uncertainties were shown by 90% confidence intervals that were derived based on a bias-adjusted approximation of the covariance matrix. We used the coefficient of determination and the Akaike Information Criterion (AIC; Zuur *et al.*, 2009) to compare the models. Analyses were conducted using the "mgcv" package (Wood, 2019) within the R environment (R Core Team, 2019). To be consistent in dealing with the specimens of different ages at capture, we only used data up to the youngest specimen captured among the Spring- and Summer-spawned cohorts (110 days).

The gradient forest method, allowing inclusion of multiple and potentially correlated variables as predictors, was used to quantify the relationships between daily increment widths and environmental variables and to describe how the daily increment widths changed in response to environmental variables (Ellis *et al.*, 2012). Along with other measures, gradient forests provide the goodness-of-fit measure R_f^2 for each response variable *f* and the importance weighted by R_f^2. We ran the gradient forests for 1000 times to obtain the variability of R_f^2 and the best run with the highest overall performance (R^2) was then used for further analysis. Analysis were conducted using the "gradientForest" package (http://gradientforest.r-forge.r-project.org/). For each cohort, the average otolith daily increment widths were used as response variables while environmental variables in three sampling regions were used as predictors.

Results

Hatching date and daily growth pattern

Hatching date of largehead hairtail in our samples ranged from December 2016 to April 2018

206 (Fig. 3). The analysis showed that the dominant spawning months in three sampling regions were
207 March to July (Fig. 3). In the following analysis, we focus on Spring-spawned cohort and
208 Summer-spawned cohort.

209 The two spawning cohorts showed obvious differences in growth patterns and overall growth
210 rates, both between seasons within a region and among the three regions (Fig. 4). Samples of the
211 Spring-spawned cohort from QD displayed a different temporal growth pattern compared with other
212 regions and times, showing two distinct growth peaks; the first peak in early May showed a lower
213 early maximum than DL and ZH, and another peak occurred in mid-August (Fig. 4a). For the
214 Summer-spawned cohort, the daily growth in ZH was substantially higher than in DL and QD; in
215 particular, fish from ZH maintained fast daily growth longer than those from DL and QD (Fig. 4b).

216 **Age-dependent growth patterns**

217 For both spawning cohorts, daily increment widths rapidly increased during the first ~40 days
218 after hatching, with growth thereafter markedly decelerating (spring) or slightly
219 decelerating/levelling off (summer) (Fig. 5).

220 Based on the qualitative change from accelerating to decelerating growth in terms of daily
221 increment widths, we focus on early growth in two phases. In the following, we will refer the first
222 40 days to as the larval period and the days 41–110 as the early juvenile period (see the Discussion
223 for justification of this terminology).

224 Across all sampling regions and different growth period (i.e., larval and juvenile), the model that
225 allowed for region-specific age-dependence of growth (Model2) provided a better description of the
226 data than the model assuming the same age-dependence growth across regions (Model1) (Table 2).

However, the model improvement in terms of both variance explained (R^2) and the Akaike Information Criterion (AIC) was markedly higher for the early juvenile period (days 41–110) compared to the larval period (first 40 days), suggesting that habitat-specific influences become prominent only during the juvenile period. This is confirmed by visual inspection of the fitted age-dependent growth effect (Fig. 6). The growth pattern among three sampling regions for the larval period is very similar (Fig. 6a and 6c) while growth pattern during juvenile period is relatively diverse (Fig. 6b and 6c). Therefore, in the following, we will focus on environmental influences on the juvenile stage of YoY largehead hairtail.

Average growth for the Spring-spawned cohort was homogenous across the regions during the larval stage, while for the juvenile stage, samples from QD displayed slower growth in comparison to DL (Table 3). For the Summer-spawned cohort, samples from ZH showed consistently faster growth than those from DL.

Relative importance of environmental variables

The daily increment width showed different patterns among the three regions (Fig. 7). The daily increment width of the Summer-spawned cohort in DL declined slowly compared with Spring-spawned cohort, at the time (around August–September) that corresponds with the weak vertical temperature gradient (difference between sea surface and bottom temperatures, TD; Fig. 7a). Samples from QD showed two peaks for the Spring-spawned cohort. The daily increment widths increased in presence of frequent northward alongshore current from June to August, as shown by the positive v (Fig. 7b) and coinciding with the decrease of sea surface salinity (SSS). In addition, the transition time to a relatively slow growth corresponds well with the decrease of TD

for the Summer-spawned cohort in QD (Fig. 7b). In ZH, the Summer-spawned cohort maintained fast daily growth rate around September and October in ZH (Fig. 7c). The time corresponds with the disappearance of the northward alongshore current and its turn southward.

The gradient forest analysis identified sea bottom temperature (SBT), TD and SSS as the most important environmental variables for explaining daily increment widths at ages 41-110 days in all sampling regions at times, although their rankings differed (Fig. 8). SBT is the most important variable in Spring-spawned cohort while TD is the most important variable in Summer-spawned cohort. The relative rankings and importance of TD and SSS vary but do not appear systematically different for Spring-spawned cohorts. In summer-spawned cohorts, SBT is the second important variable in QD and ZH but TD in DL (Fig. 8d). The velocities *u* and *v* appear consistently less important except for Summer-spawned cohort in ZH (Fig. 8f).

The gradient forest quantified the relationship between environmental variables and daily increment widths in Spring- and Summer-spawned cohorts. For the Spring-spawned cohort, otolith daily increment widths in QD and ZH show strong threshold responses to SBT at around 11.5°C and 18.5°C while in DL, there was only a relatively small threshold at around 7°C (Fig. 9). A second strong threshold response for SBT in DL occurs at around 12°C. Daily increment widths in QD were strongly influenced by TD at around 5°C. In DL, there were two less marked threshold responses to TD at around 2°C and 6°C. The strongest threshold response to SSS was seen in QD at about 29.3 and 29.5 in ZH. For the Summer-spawned cohort, daily increment widths had distinct threshold responses to SBT at around 19°C, 21°C for DL and QD, respectively (Fig. 9). Otolith daily increment widths is strongly influenced by TD at around 4°C, 2°C in DL and QD (Fig. 9). A

269 strong threshold response to SSS was seen around 27.8, 27.6 and 26 in DL, QD and ZH. In general,
270 threshold responses of daily increment widths were more evident in DL and QD compared to ZH.
271

272 ## Discussion

273 The present study explored the spawning characteristics and daily growth of YoY largehead
274 hairtail as revealed by otolith microstructure analysis in the China Seas between 29° and 39° N,
275 covering Bohai Sea, Yellow Sea and East China Sea. We back-calculated the hatching dates to
276 investigate seasonality of spawning and daily growth patterns in three sampling regions. Latitudinal
277 differences in the early growth patterns and their responses to environmental variables suggested
278 flexibility and adaptive capacity of early growth in face of environmental change. In addition, the
279 spatial and temporal differences in the early growth process response to environmental variables
280 was explored to understand the recruitment dynamics of largehead hairtail.

281 The daily increment widths of all cohorts increased and reached a peak at around 40 days of age.
282 Because seasonal patterns in growth can potentially represent both age-related, inherent variation in
283 growth as well as extrinsic seasonal variation in the ambient environment, or a combination thereof,
284 we specifically investigated the growth patterns for the period before and after the 40^{th} day.
285 Previous studies have indicated that the change from accelerating to decelerating growth is
286 associated with the transition from larval to juvenile stage (Correia *et al.*, 2002; Liao and Qu, 2008).
287 During the first 40 days, the growth in the three sampling regions was similar, showing comparable
288 growth rates and similar accelerating trends, despite great hydrological and ecological differences
289 among the regions (Fig.6 and Fig. 7). This suggests that growth during the first 40 days is

290 constrained by physiology rather than the environment, manifesting a canalized early growth
291 pattern.

292 In contrast, the growth patterns and daily growth rates over ages 41–110 days were clearly
293 different among the three sampling regions and the two seasons (Fig. 6). Therefore, two GAMM
294 models were compared to explore the influence of location on daily increment widths among three
295 sampling regions in Spring-spawned and Summer-spawned cohorts separately for larvae
296 (pragmatically defined as the first 40 days) and juveniles (41–110 days). The model that allowed for
297 region-specific growth patterns was vastly better in terms of AIC than the model assuming a
298 common growth pattern. This indicated that the environmental influences on daily increment widths
299 over 41–110 days were more marked compared to the first 40 days, suggesting more
300 habitat-specific influences rather than inherent growth influences over 41–110 days and more
301 inherent growth rather than strong environmental effects in the first 40 days (Table 2) (e.g.
302 Wullschleger and Jokela, 1999; Scharsack *et al.*, 2007). Therefore, we focus on the growth at ages
303 41–110 days and the associated environmental variables on both spatial and temporal scales.

304 **Adaptive capacity in response to food availability and environment**

305 The catches of largehead hairtail have been on the rise in Bohai Sea, Yellow Sea and East China
306 Sea, despite continued high levels of exploitation, which implies that the populations have been able
307 to maintain sufficient levels of recruitment. This suggests high adaptive capacity of larval and
308 juvenile largehead hairtail that face highly variable oceanographic conditions over seasons and the
309 latitudinal gradient from subtropical south to temperate north.

310 It is commonly hypothesized that recruitment is enhanced by responses to the oceanographic

311 conditions such as larval retention areas with favorable water temperature and food availability (e.g.
312 Beaugrand and Kirby, 2010; Ljunggren *et al.*, 2010; Morgan *et al.*, 2013; Schismenou *et al.*, 2016).
313 In this study, the three environmental variables consistently identified by the gradient forest method
314 as most important for explaining otolith growth over 41–110 days were SBT, TD and SSS in all
315 three sampling regions (Fig. 8). The preeminence of SBT (and TD to a lesser degree) is consistent
316 with the life history of largehead hairtail as YoY largehead hairtail occur near the sea floor and
317 mostly around coastal areas (Xu and Chen, 2015).

318 In coastal areas of Bohai Sea and Yellow Sea, tide is the dominant hydrodynamics and the
319 tidal-induced mixing, currents or residual currents seems to have significant effects on the
320 environmental factors. However, the tidal dynamics is not considered in NEMO and thus may cause
321 some uncertainties in the modelled environmental factors. The development of a robust
322 hydrodynamic model with tidal dynamics included is imperative, which may be much more
323 appropriate for future studies. As an initial step, the environmental variables considered in this
324 study are sufficient from the perspective of the sampling regions (DL in the Bohai Sea and QD in
325 the Yellow Sea). Specifically, DL is mainly influenced by Yellow River estuary. Thus, what
326 influence the early growth of largehead hairtail are variation in the Yellow River effluent and
327 circulation in Bohai Sea which are represented by the change of the longitudinal velocity
328 component u and the vertical temperature gradient TD. For the sampling region QD, the early
329 growth of largehead hairtail is influenced by northward alongshore current, which can be illustrated
330 by the latitudinal velocity component v and sea surface salinity (SSS). For the Spring-spawned and
331 Summer-spawned cohorts, the daily growth in DL was generally greater than in QD (Fig. 4a).

Meanwhile, the daily increment width in DL in the Summer-spawned cohort declined slowly with the decrease of TD, which may reflect the strengthening of water mixing (Fig. 7a). The early growth pattern in DL may relate to its proximity to the Yellow River estuary. DL is also near the frontal area of the Yellow Sea Cold Water Mass, which may further contribute to conditions favoring increased phytoplankton production and early growth.

Largehead hairtail from QD displayed a different growth pattern compared with DL and ZH and showed two peaks in the Spring-spawned cohort (Fig. 4a). The daily increment width of the first peak showed a lower early maximum than the peak in DL and ZH, but another peak occurred in mid-August, coinciding with the existence of a northward alongshore current, as illustrated by positive *v* (Fig. 7b). Furthermore, the fast growth pattern in QD around July–August corresponds well with the decrease of SSS. These findings indicate that the North Jiangsu Coastal Current was bringing Yangtze River Diluted Water and its abundant nutrient supply to the fishing ground in QD, with the resulting positive influence on the early growth of QD largehead hairtail population. For the Summer-spawned cohort of QD, the daily increment widths declined slowly along with the decrease of TD, which can reflect the features of alongshore current (Fig. 7b).

The daily growth in ZH was generally greater than in DL and QD for the Summer-spawned cohort, with the juveniles maintaining fast daily growth rate longer than in DL and QD (Fig. 4b). Meanwhile, northward alongshore current shifted to southward direction, bringing abundant nutrients from Yangtze River to the fishing grounds during this period (Fig. 7c).

Taken together, these results suggest that the early growth of the YoY largehead hairtail is strongly influenced not only by temperature but also by food availability. The adaptive capacity of

353 individuals from different sampling regions allows the larvae and juveniles to recruit to the
354 population successfully, despite contrasting environmental conditions.

355 Food availability can positively influence fish population dynamics by promoting early growth,
356 which has been linked to a greater ability to escape predation through outgrowing the predators and
357 thus resulting in greater overall survival (Bailey and Houde, 1989; Leggett and Deblois, 1994).
358 Water temperature also has an important influence on the early growth process of largehead hairtail
359 (Laurel *et al.*, 2017; Koenker *et al.*, 2018). The increase of water temperature is beneficial for
360 primary production, and further, for the growth and reproduction of fish species (Wang *et al.*, 2011).
361 Despite the different environmental conditions among three sampling areas, the adaptive capacity of
362 early growth response to food availability and water temperature was enhanced to sustain high yield
363 of largehead hairtail under the sustained high fishing pressure in the China Seas.

364 In conclusion, we have shown that the two spawning cohorts had obvious latitudinal differences
365 in early growth patterns, with the fastest growth in the south. The influence of location on daily
366 growth among three sampling regions suggested more physiologically constrained growth during
367 the larvae stage and stronger habitat-specific influences during juvenile stage. SBT, TD and SSS
368 were identified as important environmental factors in determining the early growth of largehead
369 hairtail in juvenile stage, probably through their influences on the quantity and distribution of food.
370 We suggest that the enhanced nutrient supply, resulting from strengthened alongshore current,
371 Yellow Sea Cold Water Mass, and Yangtze River Runoff, contribute to fast early growth of
372 largehead hairtail. Latitudinal differences in the early growth pattern and their response to
373 environmental variables suggest a high degree of plasticity and adaptive capacity of early growth.

374 Our results help to explain the resilience of largehead hairtail in face of environmental change and
375 provide a reason for high yield under continued intensive fisheries exploitation.
376

377 Acknowledgements

378 This work was supported by the National Natural Science Foundation of China (grant number:
379 41861134037) and the Research Council of Norway (grant number: 288037). We also acknowledge
380 the assistance provided by the Institute of Oceanography at the National Taiwan University and
381 Department of Marine Biotechnology and Resources at the National Sun Yat-sen University.
382

383 Conflict of interests

384 The authors state that there are no conflicts of interest to declare.
385

386 Author contributions

387 The listed authors have made substantial contributions to conception and design, acquisition of
388 data, and analysis and interpretation of data. Peng Sun, Qi Chen, Chi Zhang and Zhenjiang Ye
389 completed the otolith experiments and got the age data. Jianchao Li, Haiqing Yu and Yang Liu
390 provided the environmental data and suggestions about marine environmental variables. Caihong Fu,
391 Yi Xu, Runlong Sun and Mikko Heino designed and tested the used models. Peng Sun, Mikko
392 Heino and Yongjun Tian compiled and drafted the manuscript, while all other authors have
393 reviewed and revised it. All authors have given final approval of this manuscript.
394

Data availability statement

The data that support the findings of this study are available from the corresponding author upon reasonable request.

ORCID

Peng Sun https://orcid.org/0000-0002-0839-1785

Reference

Bailey, K. M., & Houde, E. D. (1989). Predation on eggs and larvae of marine fishes and the recruitment problem. *Advance in Marine Biology*, 25, 1-83. doi: 10.1016/S0065-2881(08)60187-X.

Bao, X. W., Li, N., Wu, D. X. (2010). Observed characteristics of the North Yellow Sea water masses in summer. Chinese Journal of Oceanology and Limnology, 28, 160-170. doi: 10.1007/s00343-010-9034-1. in Chinese with English abstract.

Baumann, H., Grohsler, T., Kornilovs, G., Makarchouk, A., Feldmann, V., Temming, A. (2006). Temperature-induced regional and temporal growth differences in Baltic young-of-the-year sprat *Sprattus sprattus*. Marine Ecology Progress Series, 317, 225-236. doi: 10.3354/meps317225.

Baumann, H., Hinrichsen, H. H., Voss, R., Stepputtis, D., Grygiel, W., Clausen, L. W., Temming, A. (2003). Linking growth to environmental histories in central Baltic young-of-the-year sprat, *Sprattus sprattus*: an approach based on otolith microstructure analysis and hydrodynamic

modeling. Fisheries Oceanography, 155, 465-476. doi: 10.1111/j.1365-2419.2005.00395.x.

Beaugrand, G., & Kirby, R. R. (2010). Climate, plankton and cod. Global Change Biology, 16, 1268-1280. doi: 10.1111/j.1365-2486.2009.02063.x.

Bergenius, M., Meekan, M., Robertson, R., McCormick, M. (2002). Larval growth predicts the recruitment success of a coral reef fish. Oecologia, 131, 521-525. doi: 10.2307/4223286.

Buckel, J. A., Steinberg, N. D., Conover, D. O. (1995). Effects of temperature, salinity, and fish size on growth and consumption of juvenile bluefish. Journal of Fish Biology, 47, 696-706. doi: 10.1111/j.1095-8649.1995.tb01935.x.

Campana, S. (2001). Accuracy, precision and quality control in age determination, including a review of the use and abuse of age validation methods. Journal of Fish Biology, 59, 197-242. doi: 10.1006/jfbi.2001.1668.

Chen, Y. L., Wang, F., Bai, X. Z., Bai, H., Ji, F. Y. (2004). Relationship between hairtail (*Trichiurus haumela*) catches and marine hydrologic environmental in East China Sea. Oceanologia et Limnologia Sinica, 35, 404-412. doi: 10.3321/j.issn:0029-814X.2004.05.003. in Chinese with English abstract.

Correia, A. T., Antunes, C., Coimbra, J. (2002). Aspects of the early life history of the Europe conger eel (*Conger conger*) inferred from the otolith microstructure of metamorphic larvae. Marine Biology, 140, 165-173. doi: 10.1007/s002270100678.

Cowen, R. K., & Sponaugle, S. (2009). Larval dispersal and marine population connectivity. Annual Review of Marine Science, 1, 443-466. doi: 10.1146/annurev.marine.010908.163757.

Denit, K., & Sponaugle, S. (2004). Growth variation, settlement, and spawning of Gray Snapper

437 across a latitudinal gradient. Transactions of the American Fisheries Society, 133, 1339-1355.
438 doi: 10.1577/T03-156.1.
439 Donlon, C. J., Martin, M., Stark, J., Roberts-Jones, J., Fiedler, E., Wimmer, W. (2012). The
440 operational sea surface temperature and sea ice analysis (OSTIA) system. Remote Sensing of
441 the Environment, 116, 140-158. doi: 10.1016/j.rse.2010.10.017.
442 Ellis, N., Smith, S. J., Pitcher, C. R. (2012). Gradient forests: calculating importance gradients on
443 physical predictors. Ecology, 93, 156-168. doi: 10.1890/11-0252.1.
444 Fedewa, E. J., Miller, J. A., Hurst, T. P., Jiang, D. (2017). The potential effects of pre-settlement
445 processes on post-settlement growth and survival of juvenile northern rock sole
446 (*Lepidopsetta polyxystra*) in Gulf of Alaska nursery habitats. Estuarine, Coastal and Shelf
447 Science, 180, 46-57. doi: 10.1016/j.ecss.2017.02.028.
448 Gallagher, B. K., Hice, L. A., McElroy, A. E., Cerrato, R. M., Frisk, M. G. (2015). Factors
449 influencing daily growth in young-of-the-year winter flounder along an urban gradient
450 revealed using hierarchical linear models. Marine and Coastal Fisheries: Dynamics,
451 Management and Ecosystem Science, 7, 200-219. doi: 10.1080/19425120.2015.1020175.
452 Gu, Y. H., & Xiu, R. C. (1996). On the current and storm flow in the Bohai Sea and their role in
453 transporting deposited silt of the Yellow River. Journal of Oceanography of Huanghai & Bohai
454 Seas, 14, 1-6. in Chinese with English abstract.
455 Hjort, J. (1914). Fluctuations in the great fisheries of northern Europe viewed in the light of
456 biological research. Rapports et Procès-Verbaux des Réunions, 20, 1-228.
457 Houde, E. D. (1987). Fish early life dynamics and recruitment variability. American Fisheries

458 Society Symposium, 2, 17-29.

459 Houde, E. D. (1989). Comparative growth, mortality, and energetics of marine fish larvae:
460 temperature and implied latitudinal effects. Fishery Bulletin, 87, 471-495.

461 Houde, E. D., & Zastrow, C. E. (1993). Ecosystem- and taxon-specific dynamic and energetics
462 properties of larval fish assemblages. Bulletin of Marine Science, 53, 290-335.

463 Hughes, J. M., Stewart, J., Lyle, J. M., McAllister, J., Stocks, J. R., Suthers, I. M. (2017). Influence
464 of latitudinal variation in environmental gradients and population structure on the demography
465 of a widespread pelagic fish, Arripis trutta (Forster, 1801). Environmental Biology of Fishes,
466 100, 121-135. doi: 10.1007/s10641-016-0565-y.

467 Husebø, A., Slotte, A., Stenevik, E. K. (2007). Growth of juvenile Norwegian spring-spawning
468 herring in relation to latitudinal and interannual differences in temperature and fish density in
469 their coastal and fjord nursery areas. ICES Journal of Marine Science, 64, 1161-1172. doi:
470 10.1093/icesjms/fsm081.

471 Ji, Y. P., Liu, Q., Liao, B. C., Zhang, Q. Q., Han, Y. N. (2019). Estimating biological reference
472 points for Largehead hairtail (*Trichiurus lepturus*) fishery in the Yellow Sea and Bohai Sea.
473 Acta Oceanologica Sinica, 38, 20-26. doi: 10.1007/s13131-019-1343-4.

474 Johnson, R. B., Grimes, C. B., Royer, C. F., Donohoe, C. J. (2007). Identifying the contribution of
475 wild and hatchery Chinook salmon (*Oncorhynchus tshawytscha*) to the ocean fishery using
476 otolith microstructure as natural tags. Canadian Journal of Fisheries and Aquatic Sciences, 64,
477 1643-1692. doi: 10.1139/F07-129.

478 Kingsford, M. J., Hughes, J. M. (2005). Patterns of growth, mortality and size of the tropical

damselfish Acanthochromis polyacanthus across the continental shelf of the Great Barrier Reef. Fishery Bulletin, 103, 561-573. doi: 10.1111/j.1444-2906.2005.01082.x.

Koenker, B. L., Laurel, B. J., Copeman, L. A., Ciannelli, L. (2018). Effects of temperature and food availability on the survival and growth of larval Arctic cod (*Boreogadus saida*) and walleye pollock (*Gadus chalcogrammus*). ICES Journal of Marine Science, doi: 10.1093/icesjms/fsy062.

Köster, F. M. Hinrichsen, H. H., Schnack, D., St John, M. A., MacKenzie, B. R., Tomkiewicz, J., Möllmann, C., Kraus, G., Plikshs, M., Makarchouk, A., Aro, E. (2003). Recruitment of Baltic cod and sprat stocks: identification of critical life stages and incorporation of environmental variability into stock-recruitment relationships. Scientia Marina, 67, 129-154. doi: 10.1007/978-1-4615-3428-0_27.

Laurel, B. J., Copeman, L. A., Spencer, M., Iseri, P. (2017). Temperature-dependent growth as a function of size and age in juvenile Arctic cod (*Boreogadus saida*). ICES Journal of Marine Science, 74, 1614-1621. doi: 10.1007/s00300-015-1761-5.

Leggett, W. C., & Deblois, E. (1994). Recruitment in marine fishes: is it regulated by starvation and predation in the egg and larval stages? Netherlands Journal of Sea Research, 32, 119-134. doi: 10.1016/0077-7579(94)90036-1.

Lett, C., Ayata, S. D., Huret, M., Irisson, J. O. (2010). Biophysical modelling to investigate the effects of climate change on marine population dispersal and connectivity. Progress in Oceanography, 87, 106-113. doi: 10.1016/j.pocean.2010.09.005.

Li, G. X., Han, X. B., Yue, S. H., Wen, G. Y., Yang, R. M., Kusky, T. M. (2006). Monthly

variations of water masses in the East China Seas. *Continental Shelf Research*, 26, 1954-1970. doi: 10.1016/j.csr.2006.06.008.

Liao, R., & Qu, Y. J. (2008). Present status of studies and applications on otolith of fishes. South China Fisheries Science, 4, 69-75. doi: 10.3969/j.issn.2095-0780.2008.01.013. in Chinese with English abstract.

Lin, L., Zheng, Y., Cheng, J., Liu, Y., Ling, J. (2006). A preliminary study on fishery biology of main commercial fishes surveyed from the bottom trawl fisheries in the East China. Marine Science, 30, 21-25. doi: 10.3969/j.issn.1000-3096.2006.02.005. in Chinese with English abstract.

Lin, X. H., & Zhang, D. W. (1999). Inference in generalized additive mixed models by using smoothing splines. Journal of the Royal Statistical Society. Series B, 61, 381-400. doi: 10.2307/2680648.

Liu, Y., Cheng, J. H., Chen, Y. (2009). A spatial analysis of trophic composition: a case study of hairtail (*Trichiurus japonicus*) in the East China Sea. Hydrobiologia, 632, 79-90. DOI: 10.1007/s10750-009-9829-2.

Ljunggren, L., Sandström, A., Bergström, U., Mattila, J., Lappalainen, A., Johansson, G., Sundblad, G., Casini, M., Kalijuste, O., Eriksson, B. K. (2010). Recruitment failure of coastal predatory fish in the Baltic Sea coincident with an offshore ecosystem regime shift. ICES Journal of Marine Science, 67, 1587-1595. doi: 10.1093/icesjms/fsq109.

Lowerre-Barbieri, S., DeCelles, G., Pepin, P., Catalán, I. A., Muhling, B., Erisman, B., Tringali, M. D. (2017). Reproductive resilience: A paradigm shift in understanding spawner–recruit

systems in exploited marine fish. Fish and Fisheries, 18, 285–312. doi: 10.1111/faf.12180.

Mallo, M., Ziveri, P., Mortyn, P. G., Schiebel, R., Grelaud, M. (2016). Low panktic foraminiferal diversity and abundance observed in a 2013 West-East Mediterranean Sea transect. Biogeosciences Discussions, doi: 10.5194/bg-2016-266.

Mesa, M. L. (2007). The utility of otolith microstructure in determining the timing and position of the first annulus in juvenile Antarctic toothfish (*Dissostichus mawsoni*) from the South Shetland Islands. Polar Biology, 30, 1219-1226. doi: 10.1007/s00300-007-0281-3.

Mi, T. Z., Yao, Q. Z., Meng, J., Zhang, X. L., Liu, S. M. (2012). Distributions of nutrients in the Southern Yellow Sea and East China Sea in spring and summer 2011. Oceanologia et Limnologia Sinica, 43, 678-688. in Chinese with English abstract.

Miller, T. J., Crowder, L. B., Rice, J. A., Marschall, E. A. (1988). Larval size and recruitment mechanisms in fishes: toward a conceptual framework. Canadian Journal of Fisheries and Aquatic Sciences, 45, 1657-1670. doi: 10.1139/f88-197.

Morgan, E., ÓRiordan, R. M., Culloty, S. C. (2013). Climate change impacts on potential recruitment in an ecosystem engineer. Ecology and Evolution, 3, 581-594. doi: 10/1002/ece3.419.

Morse, W. W. (1989). Catchability, growth and mortality of larval fishes. Fishery Bulletin, 87, 417-446. doi: 10.1016/0165-7836(89)90042-8.

Munday, P. L., Leis, J., Lough, J., Paris, C., Kingsford, M., Berumen, M., Lambrechts, J. (2009). Climate change and coral reef connectivity. Coral Reefs, 28, 379-395.

Neubauer, P., Jensen, O. P., Hutchings, J. A., Baum, J. K. (2013). Resilience and recovery of

overexploited marine populations. Science, 340, 347-349. doi: 10.1126/science.1230441.

Neuman, M. J., Witting, D. A., Able, K. W. (2001). Relationships between otolith microstructure, otolith growth, somatic growth and ontogenetic transitions in two cohorts of windowpane. Journal of Fish Biology, 58, 967-984. doi: 10.1111/j.1095-8649.2001.tb00548.x.

Otterlei, E., Nyhammer, G., Folkvord, A., Stefansson, S. O. (1999). Temperature- and size-dependent growth of larval and early juvenile Atlantic cod (*Gadus morhua*): a comparative study of Norwegian coastal cod and northeast Arctic cod. Canadian Journal of Fisheries and Aquatic Sciences, 56, 2099-2111. doi: 10.1139/cjfas-56-11-2099.

R Core Team. (2019). R: a language and environment for statistical computing. R Foundation for Statistical Computing, Vienna, Austria Retrieved from. https://www.R-project.org/.

Rozema, P. D., Biggs, T., Sprong, P. A. A., Buma, A. G. J., Venables, H. J., Evans, C., Meredith, M. P., Bolhuis, H. (2017). Summer microbial community composition governed by upper-ocean stratification and nutrient availability in northern Marguerite Bay, Antarctica. Deep Sea Research Part Ⅱ Topical Studies in Oceanography, 139, 151-166.

Rupert, D., Wand, M. P., Carroll, R. J. (2003). Semiparametric regression. New York, NY: Cambridge University Press.

Ruttenberg, B. I., Haupt, A. J., Chiriboga, A. I., Warner, R. R. (2005). Patterns, causes and consequences of regional variation in the ecology and life history of a reef fish. Oecologia, 145, 394-403. doi: 10.2307/20062430.

Scharsack, J. P., Kalbe, M., Harrod, C., Rauch, G. (2007). Habitat-specific adaptation of immune responses of stickleback (*Gasterosteus aculeatus*) lake and river ecotypes. Proceedings of the

563 Royal Society B: Biological Sciences, 274, 1523-1532. doi: 10.1098/rspb.2007.0210.
564 Schismenou, E., Palmer, M., Giannoulaki, M., Alvarez, I., Tsiaras, K., Triantafyllou, G., Somarakis,
565 S. (2016). Seasonal changes in otolith increment width trajectories and the effect of
566 temperature on the daily growth rate of young sardines. Fisheries Oceanography, 25, 362-372.
567 doi: 10.1111/fog.12158.
568 Shoji, J. (2005). Distribution, feeding condition and growth of Japanese Spanish mackerel
569 (*Scomberomorus niphonius*) larvae in the Seto Inland Sea. Fish Bulletin, 103, 371-379.
570 Sogard, S. M. (2011). Interannual variability in growth rates of early juvenile sablefish and the role
571 of environmental factors. Bulletin of Marine Science, 87, 857-872.
572 Spurr, A. R. (1969). A low-viscosity epoxy resin embedding medium for electron microscopy.
573 Journal of Ultrastructure Research, 26, 31-43. doi: 10.1016/S0022-5320(69)90033-1.
574 Stearns, S. C. (1992). The evolution of life histories. Oxford University Press, Oxford.
575 Stevenson, D. K., & Campana, S. E. (1992). Otolith microstructure examination and analysis.
576 Canadian Special Publication of Fisheries and Aquatic Sciences, 117. doi:
577 10.1007/BF00043932.
578 Sun, P., Chen, Q., Fu, C.H., Zhu, W.B., Li, J.C., Zhang, C., Yu, H.Q., Sun, R.L., Xu,Y., Tian, Y. J.
579 (2020). Daily growth of young-of-the-year largehead hairtail (*Trichiurus japonicus*) in relation
580 to environmental variables in the East China Sea. Journal of Marine Systems. doi:
581 10.1016/j.jmarsys.2019.103243.
582 Takahashi, M., McCormick, M. I., Munday, P. L., Jones, G. P. (2012). Influence of seasonal and
583 latitudinal temperature variation on early life-history traits of a coral reef fish. Marine and

584 Freshwater Research, 63, 856-864. doi: 10.1071/MF11278.
585 Trip, E. D. L., Clements, K. D., Raubenheimer, D., Choat, J. H. (2014). Temperature-related
586 variation in growth rate, size, maturation and life span in a marine herbivorous fish over a
587 latitudinal gradient. Journal of Animal Ecology, 83, 866-875. doi: 10.1111/1365-2656.12183.
588 Tupper, M., & Boutilier, R. G. (1995). Effects of habitat on settlement, growth, and postsettlement
589 survival of Atlantic cod (*Gadus morhua*). Canadian Journal of Fisheries and Aquatic Sciences,
590 52, 1834-1841. doi: 10.3354/meps151225.
591 Valenzuela, G. S., & Vargas, C. A. (2002). Comparative larval growth rate of *Sprattus sprattus* in
592 relation to physical and biological oceanographic features in the North Sea. Archive of Fishery
593 and Marine Research, 49, 213-230.
594 Wang, Y. Z., Jia, X. P., Lin, Z. J., Sun, D. R. (2011). Responses of Trichiurus japonicus catches to
595 fishing and climate variability in the East China Sea. Journal of Fisheries of China, 35,
596 1881-1889. doi: 10.1016/S1671-2927(11)60313-1. in Chinese with English abstract.
597 Watanabe, Y., Ochiai, S. I., Fukamichi, K. (2014). Larval growth rates differ in response to
598 seasonal temperature variations among clupeoid species inhabiting the Pacific coastal waters
599 of Japan. Fisheries Science, 80, 43-51. doi: 10.1007/s12562-013-0684-8.
600 Whitman, G. and Johnson, R. C. (2016). Imaging of otoliths for analysis of fish age and growth: a
601 guide for measuring daily increments in adult and juvenile otoliths using Image-Pro Premier.
602 University of California Davis, Center for Watershed Sciences. www.Barnett-Johnson.com
603 Wood, S. (2019). Package 'mgcv'. Version 1.8-31. Retrieve from https://cran.r-project.org/.
604 Wullschleger, E., & Jokela, J. (1999). Does habitat-specific variation in trematode infection risks

influence habitat distribution of two closely related freshwater snails? Oecologia, 121, 32-38. doi: 10.1007/s004420050904.

Xu, Z., & Chen, J. (2015). Migratory routes of *Trichiurus lepturus* in the East China Sea, Yellow Sea and Bohai Sea. Journal of Fisheries of China, 39, 824-835. in Chinese with English abstract.

Yang, Z. S., Ji, Y. J., Bi, N. S., Lei, K., Wang, H. J. (2011). Sediment transport off the Huanghe (Yellow River) delta and in the adjacent Bohai Sea in winter and seasonal comparison. Estuarine, Coastal and Shelf Science, 93, 173-181. doi: 10.1016/j.ecss.2010.06.005.

Zhang, B. (2004). Feeding habits and ontogenetic diet shift of hairtail fish (*Trichiurus lepturus*) in East China Sea and Yellow Sea. Marine Fisheries Research, 25, 6-1. in Chinese with English abstract.

Zuur, A. F., Ieno, E. N., Walker, N. J., Saveliev, A. A., Smith, G. M. (2009). GLM and GAM for count data BT-Mixed effects models and extensions in ecology with R. Springer New York, pp. 209-243. doi: 10.1007/978-0-387-87458-6.

Tables and Figures

Table1. Sampling information of Young-of-the-year largehead hairtail captured in three sampling regions: Dalian (DL), Qingdao (QD) and Zhoushan (ZH).

Sampling sea area	Sampling region	Sampling month	No. of sampled fish	Pre-anal length range (mm)	Age range (days)
Bohai Sea	DL	September, 2017	53	33-161	43-204
Bohai Sea	DL	October, 2017	14	81-154	90-187
Yellow Sea	QD	September, 2017	37	123-163	108-202
Yellow Sea	QD	October, 2017	30	64-102	69-132
Yellow Sea	QD	November, 2017	19	68-120	56-145
East China Sea	ZH	June, 2017	30	80-165	90-195
East China Sea	ZH	July, 2017	7	135-146	107-202
East China Sea	ZH	September, 2017	18	37-110	58-160
East China Sea	ZH	November, 2017	10	109-147	126-210
East China Sea	ZH	December, 2017	12	144-163	140-204
East China Sea	ZH	May, 2018	30	42-167	37-185

Table 2. Comparison of GAMM models describing the variation in daily increment widths of Spring- and Summer-spawned cohort at larval (1–40 days) and juvenile (41–110 days) stages in Dalian (DL), Qingdao (QD) and Zhoushan (ZH). Model1 assumes that the age-dependent component of growth, the smooth term in these GAMMs, is region-unspecific, whereas Model2 assumes that this effect is region-specific. R^2 values represent goodness-of-fit. ΔAIC is the AIC difference between Model1 and Model2. See the Methods for detailed specification of the models.

Cohorts	Days	R^2_{Model1}	R^2_{Model2}	ΔAIC
Spring-spawned cohort	1-40 days	0.452	0.462	36.0
	41-110 days	0.206	0.302	819
Summer-spawned cohort	1-40 days	0.406	0.410	32.3
	41-110 days	0.335	0.356	118

631 Table 3. Fixed-effect results from the GAMM analysis with Model1 and Model2 describing the daily increment
632 widths variation in Spring-spawned cohort and Summer-spawned cohort at 1-40 days and 41-110 days in
633 Dalian (DL, reference level), Qingdao (QD) and Zhoushan (ZH). Estimates correspond to mean daily growth
634 expressed at logarithmic scale. SE: standard error. See Table 2 for further explanations.

	Days	Variables	Model1			Model2		
			Estimate	SE	*p*	Estimate	SE	*p*
Spring-spawned cohort	1-40 days	(Intercept)	1.388	0.033		1.388	0.033	
		Location QD	-0.044	0.040	0.271	-0.044	0.040	0.271
		Location ZH	-0.063	0.048	0.189	-0.063	0.048	0.189
	41-110 days	(Intercept)	1.518	0.037		1.526	0.037	
		Location QD	-0.234	0.044	1.08×10^{-7}	-0.246	0.045	3.83×10^{-8}
		Location ZH	0.025	0.053	0.639	0.025	0.053	0.643
Summer-spawned cohort	1-40 days	(Intercept)	1.480	0.042		1.480	0.042	
		Location QD	-0.064	0.056	0.246	-0.064	0.056	0.246
		Location ZH	0.241	0.062	1.12×10^{-4}	0.241	0.062	1.12×10^{-4}
	41-110 days	(Intercept)	1.4945	0.049		1.475	0.048	
		Location QD	-0.069	0.064	0.282	-0.048	0.063	0.452
		Location ZH	0.328	0.072	6.13×10^{-6}	0.347	0.071	1.17×10^{-6}

635

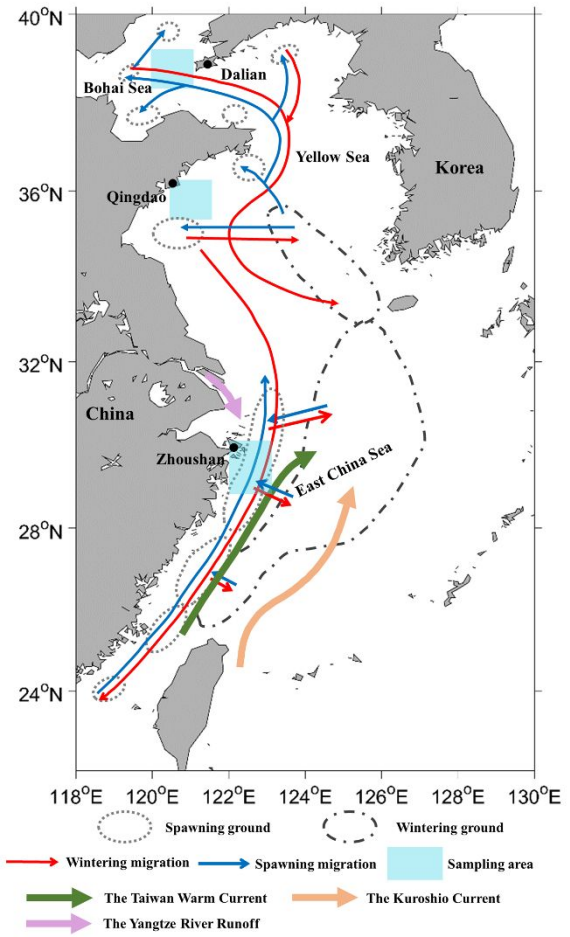

636

637 Figure 1. The study regions, main ocean currents, and migration route of largehead hairtail in the China Seas.

638

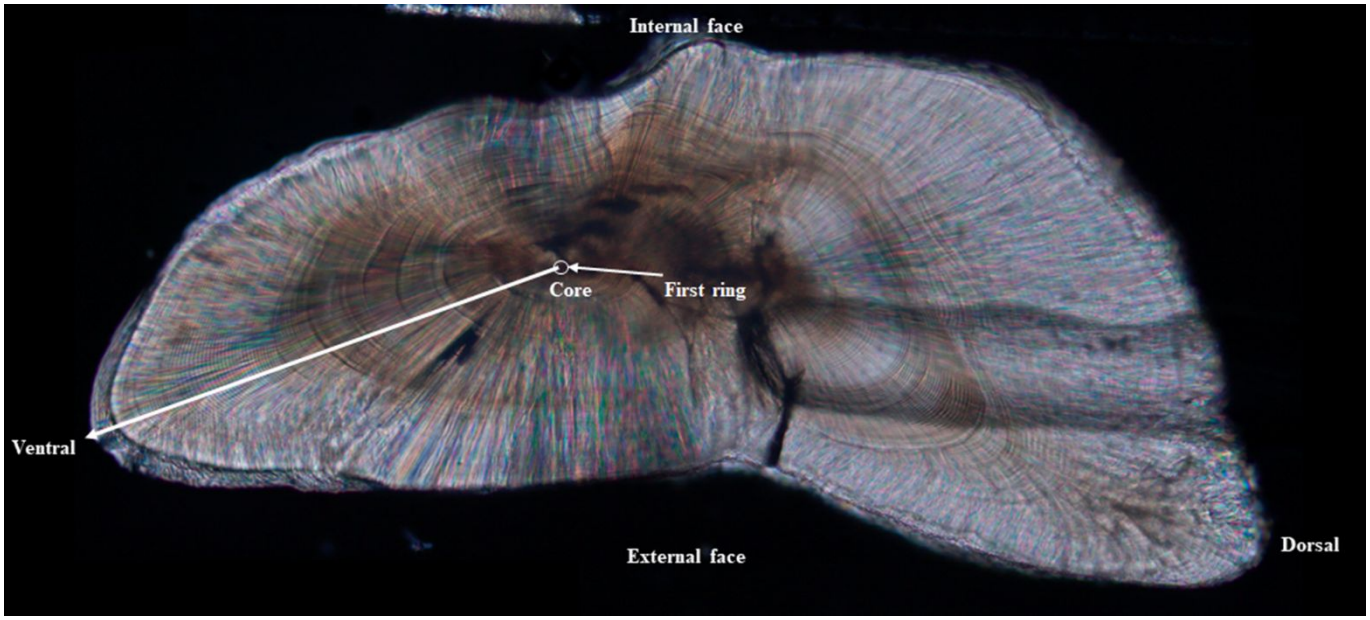

639

640 Figure 2. Polished sagittal otolith of a Young-of-the-Year largehead hairtail aged 165 days. All increments were
641 counted and measured along the same axis from core to ventral of the otolith.

642

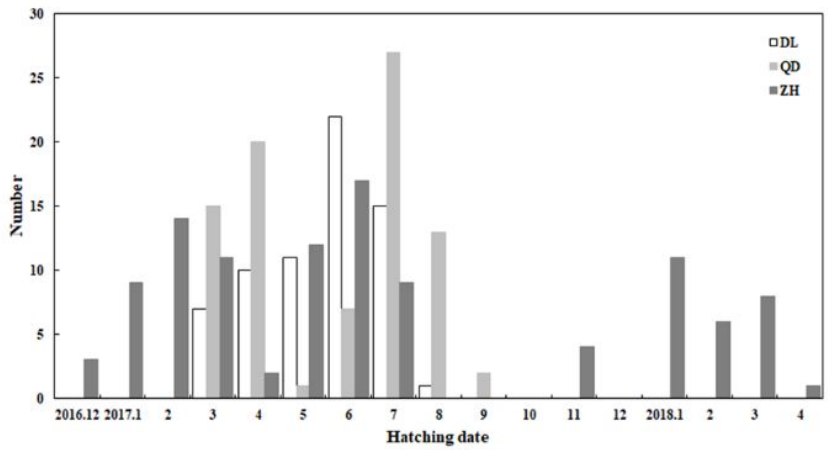

643

644 Figure 3. Distribution of Young-of-the-Year hatching date of largehead hairtail caught in three sampling regions:
645 Dalian (DL), Qingdao (QD) and Zhoushan (ZH).

646

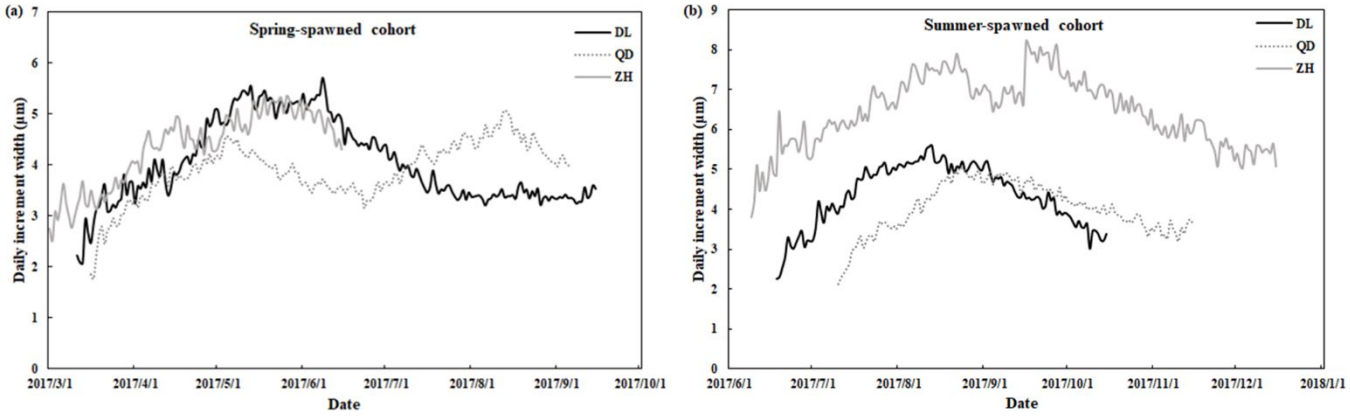

Figure 4. Daily increment width (averaged over all individuals within a cohort/region on the same date) of two spawning cohorts: (a) Spring-spawned cohort and (b) Summer-spawned cohort in 2017, in three regions: Dalian (DL), Qingdao (QD) and Zhoushan (ZH).

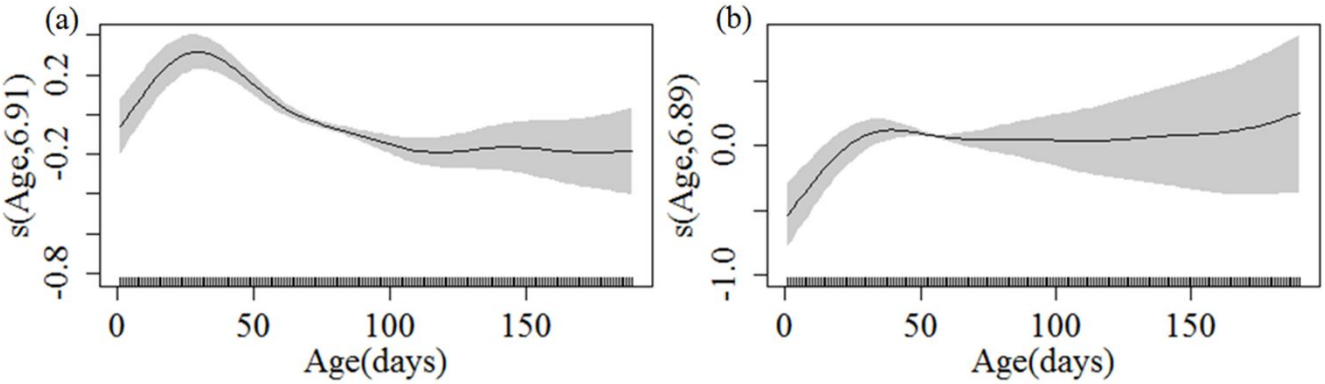

Figure 5. Generalized Additive Mixed Model fitted daily increments width over age for all specimens of two spawning cohorts: (a) Spring-spawned cohort and (b) Summer-spawned cohort. The shaded areas indicate 90% confidence interval and the ticks on x-axis indicate sampled data of spawning cohorts.

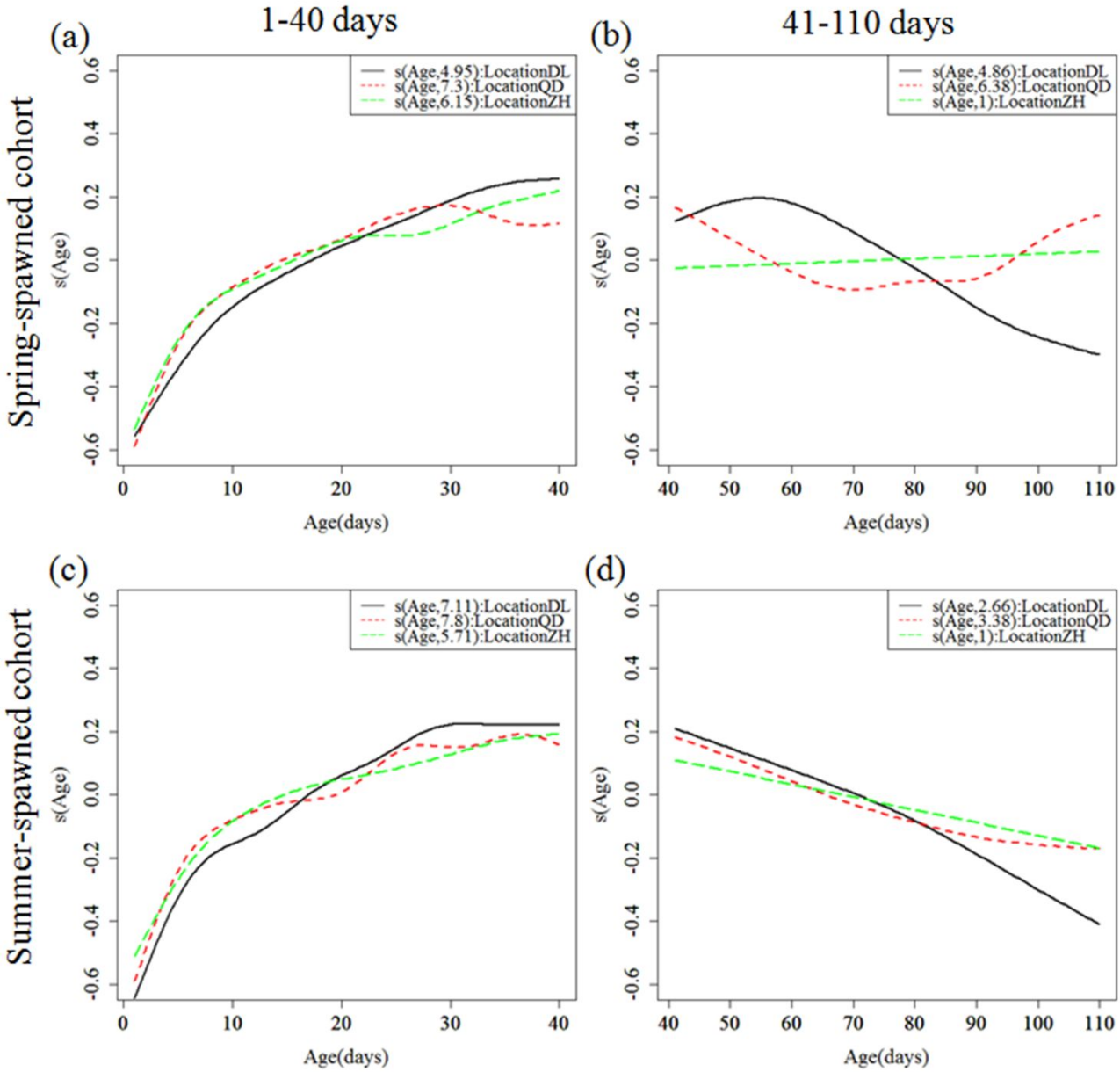

Figure 6. Smooth terms corresponding to age- and location-dependent effects in Generalized Additive Mixed Model describing otolith daily increment widths of three sampling regions for Spring- (a, b) and Summer-spawned (c, d) cohorts within two stages: the first 40 days (a, c) and 41–110 days (b, d).

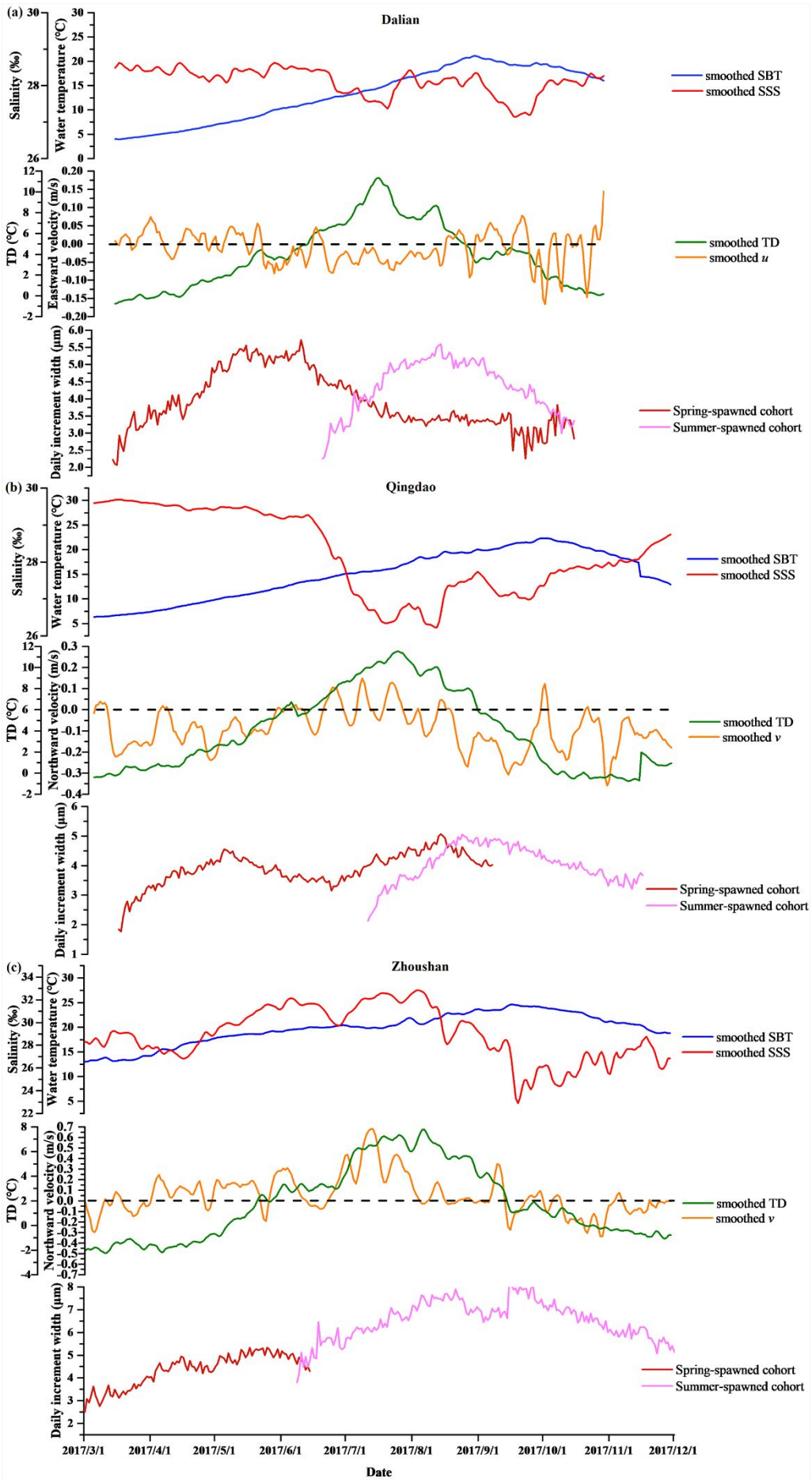
(a)
Dalian
Salinity (‰)
Water temperature (℃)
smoothed SBT
smoothed SSS
TD (℃)
Eastward velocity (m/s)
smoothed TD
smoothed u
Daily increment width (μm)
Spring-spawned cohort
Summer-spawned cohort
(b)
Qingdao
Salinity (‰)
Water temperature (℃)
smoothed SBT
smoothed SSS
TD (℃)
Northward velocity (m/s)
smoothed TD
smoothed v
Daily increment width (μm)
Spring-spawned cohort
Summer-spawned cohort
(c)
Zhoushan
Salinity (‰)
Water temperature (℃)
smoothed SBT
smoothed SSS
TD (℃)
Northward velocity (m/s)
smoothed TD
smoothed v
Daily increment width (μm)
Spring-spawned cohort
Summer-spawned cohort
2017/3/1
2017/4/1
2017/5/1
2017/6/1
2017/7/1
2017/8/1
2017/9/1
2017/10/1
2017/11/1
2017/12/1
Date

662

663 Figure 7. Daily increment width of two dominant spawning cohorts in relation to environmental variables in three
664 sampling regions: (a) Dalian (DL), (b) Qingdao (QD) and (c) Zhoushan (ZH). The environmental time series
665 of sea bottom temperature (SBT), sea surface salinity (SSS), temperature difference between sea surface and
666 bottom temperature (TD), and eastward and northward velocities (*u* and *v*) have been smoothed using 3-day
667 moving average.

668

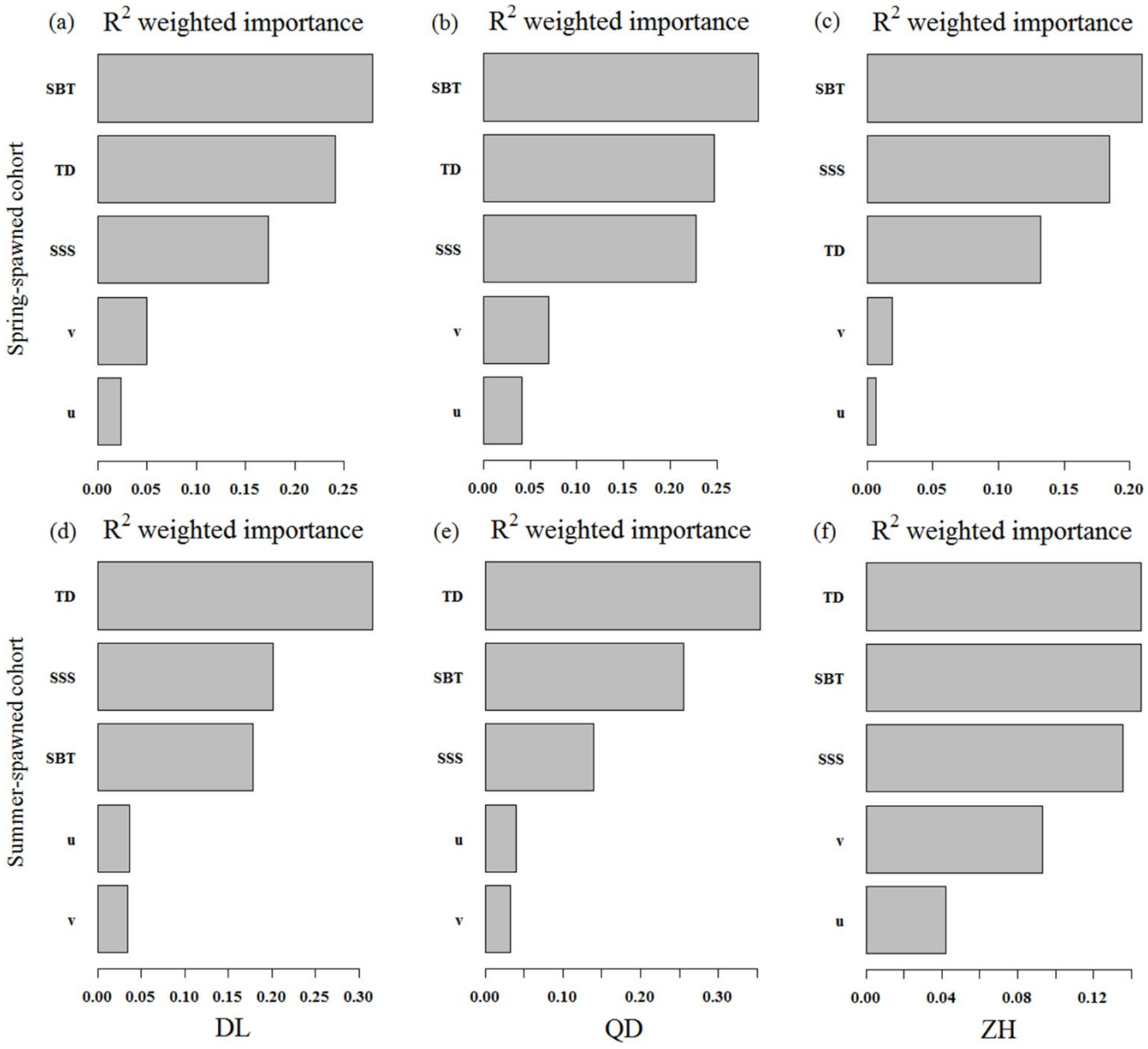

669

670 Figure 8. Importance of environmental variables, including temperature difference between sea surface and
671 bottom temperatures (TD), sea bottom temperature (SBT), sea surface salinity (SSS), and eastward and
672 northward velocities (*u* and *v*), in relation to otolith daily increment width of Spring- and Summer-spawned
673 cohorts over 41-110 days in three sampling regions, Dalian (DL), Qingdao (QD) and Zhoushan (ZH).

674

675

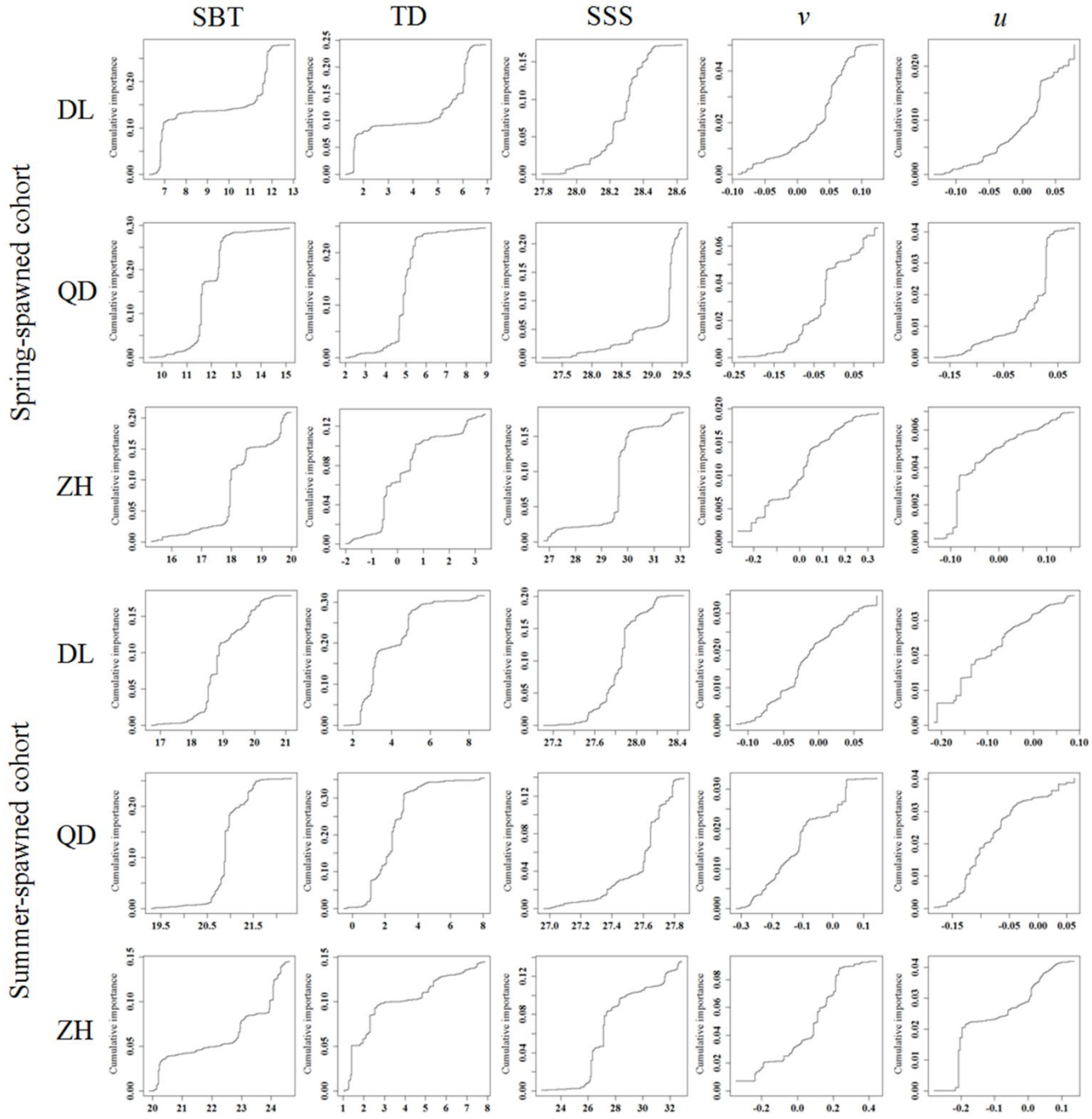

676

677 Figure 9. Cumulative importance of five environmental variables in relation to otolith daily increment of the
678 Spring-spawned cohort and Summer-spawned cohort over 41-110 days in Dalian (DL), Qingdao (QD) and
679 Zhoushan (ZH). Five columns represent the responses of otolith daily increment widths to sea bottom
680 temperature (SBT), temperature difference between sea surface temperature and bottom temperature (TD),
681 sea surface salinity (SSS), and eastward and northward velocities (*v* and *u*), respectively.

682